

Counter-intuitive comparable diffusivity of xylene isomers in zeolitic mesopores: Confirmation from adsorption and catalysis studies

Parimal A Parikh

Chemical Engineering Department, S.V. National Institute of Technology, Surat 395 007 India.

E-mail: parimal.svr@gmail.com

Received 17 February 2017; accepted 3 August 2017

The reaction of commercial interest, toluene methylation to selectively obtain *para*-xylene has been studied. For this purpose, zeolite Beta is modified to impart mesoporosity in the crystals such that formation of kinetically favourable *para*-isomer (as advocated by some schools earlier) facilitates and diffuses out easily. However, when this modification did not meet the expectation, pore openings on crystal surface have been narrowed using tetraethyl *ortho*-silicate (TEOS). Albeit, TEOS is found to enter the pores of modified zeolite and no *para*-selectivity could be attained and proportion of *meta*-isomer higher than thermodynamically determined is obtained. Catalytic- and xylene adsorption kinetic- results led to conclude (1) diffusivity of *para*-xylene is only 1.33 times higher than that of the *meta*-isomers in parent and hierarchical zeolite Beta samples and (2) extent of increase in diffusivity of *para*- and *meta*-xylene due to mesoporosity generation is comparable (about 1.14 times) unlike increase by 2 order of magnitude reported in case of ZSM-5. These observations dispel the early reckoning: large pore zeolites affording *para*-xylene selectivity in the reaction of toluene methylation.

Keywords: Aromatic alkylation, Diffusion coefficient, Mesoporous zeolite, Shape selectivity, Zeolite beta

Importance of toluene methylation reaction with an intention to selectively, produce *para*-xylene need not be over-emphasized. Many papers, including recent ones^{1,2} have described the commercial significance of and various routes for manufacturing *para*-xylene and hence are not repeated here the well-reported aspects. To increase *para*-xylene selectivity, majority of the work has employed medium pore zeolite ZSM-5 modified in variety of manners such as impregnation, silylation, etc. However, among the reports on use of ZSM-5 for toluene methylation, the one by Ahn *et al.*¹ distinctly stands out due to their attempt of generating mesoporosity in ZSM-5 and then silylating it. Silylated desilicated zeolite ZSM-5 afforded very high *para*-selectivity, however, time-on-stream (TOS) behaviour of the modified catalysts was not found in the article. Silylation is known to fine-tune the channel openings on the external surface of zeolite crystals³. Further, Yashima *et al.*⁴ observed much higher proportion of *para*-xylene (53.5%) than that dictated by thermodynamics (21.8% at their reaction temperature) on large pore zeolite HY advancing an argument that *para*- and *ortho*-xylenes are the primary products and their isomerisation to *meta*-xylene is hindered in supercages. Al-Khattaf *et al.*⁵ have observed *para*-xylene selectivity on zeolite USY at contact time of

feed with catalyst upto 15 s in a fluidized bed reactor. They employed toluene to methanol molar ratio of 1 in feed and despite that the highest conversion reported by them was only about 12% (with corresponding total xylene yield of about 10.5%) against possible 50%. It is evident that the contact time in the fluidized bed reported by them is limited by the catalyst life. Ahn *et al.*¹ observed little formation of “lighters” on zeolite Beta during toluene methylation, however, xylene isomer distribution was not given. Further, they report less than complete conversion of methanol at reaction temperature of 673K. Observations claiming *para*-selectivity over large pore zeolites particularly for toluene methylation are contrary to myriad reports that appeared subsequently showing thermodynamic distribution of isomers, i.e., no *para*-selectivity.

To passivate external surface sites (responsible for non-shape selective reactions) or to reduce channel opening cross section on external surface of zeolite crystals, depositing SiO₂ layer using compounds, e.g., tetraalkoxysilanes is well reported. Reports⁶⁻⁸ describe silylation of large pore zeolite Beta. Chun *et al.*⁶ had observed gradually reducing *m*-xylene uptake quantity over silylated zeolite Beta and thus inferring decreasing channel openings.

In light of the above described modifications performed on zeolites, it was intended to study effects of such modifications on large pore zeolite Beta, with channel cross-sections of $5.7 \text{ \AA} \times 7.5 \text{ \AA}$ and $5.6 \text{ \AA} \times 6.5 \text{ \AA}$ ⁹ in the present work. It was envisaged that with the generation of mesoporosity by treating large pore zeolite Beta, with alkaline solution and consequently enhanced acidity, it might be possible to reduce the reaction temperature for toluene methylation and thus, extent of methylation reaction could increase against other competitive reactions. However, knowing even unmodified medium pore zeolite ZSM-5 to afford predominantly undesired *meta*-xylene¹⁰, effects of narrowing the pore opening by silylation in two stages on catalysts' performance for toluene methylation was studied. Thus, the motivation behind the present work was (1) to study effects of mesoporosity and increased acidity due to desilication, and (2) pore narrowing on crystal surface of zeolite Beta on product distribution and reaction temperature requirement.

Experimental Section

Chemicals and feedstock

Toluene (MERCK, 99.8%), methanol (FINAR, 99%), sodium hydroxide pellets (FINAR, 97%), tetraethylorthosilicate (National Chemicals, 98.5%) were used as-received. Zeolite H-Beta (Si/Al = 25, crystal size 150-200 nm) was purchased from Süd-Chemie India Pvt. Ltd., Baroda, India.

Catalyst modifications

Desilication

Parent H-Beta was desilicated using 0.2 M NaOH solution (30 mL/g of catalyst) at 340 K under continuous stirring for 45 min. After cooling to room temperature, solid was filtered, washed with deionized water and dried at 383 K. The resulting solid was treated with 10 wt% ammonium nitrate solutions (15 mL/g of catalyst) three times under reflux in a round bottom flask to change to ammonium form (NH_4^+) from sodium form (Na^+). Then the solid samples obtained were again washed with deionized/distilled water and dried at 373 K, followed by calcining at 823 K for 4 h in flowing air (50 mL/min) to H form of zeolite Beta.

Silylation

This modification was accomplished by using tetraethylorthosilicate (TEOS) as a silylating agent. Solution of toluene: methanol: TEOS (47:47:6.5 mass ratio) was fed to fixed bed tubular glass reactor having

2 g catalyst with flow rate of 8 mL/h and hydrogen gas flow rate of 50 mL/min at 503 K for 2 h. Then catalyst bed was purged with nitrogen gas for 1 h at the same temperature and flow rate, followed by calcination at 823 K for 10 h. The samples obtained are named as S-H-Beta (silylated H-Beta), DS-H-Beta (double silylated H-Beta) and for desilicated parent zeolite as S-Desi-H-Beta (silylated Desilicated H-Beta), DS-Desi-H-Beta (Double silylated desilicated H-Beta).

Catalytic test

Catalytic performance of the samples was evaluated for toluene methylation (6:1 toluene to methanol molar ratio) on 2 g of catalyst in a fixed bed tubular glass reactor (25.4 mm diameter, 30 cm length, 1 g catalyst, particles of size between 0.5 and 1 mm) at temperature 673 K under 1 atmosphere pressure using hydrogen as a carrier gas (50 mL/min, H_2 /hydrocarbons 2 mol/mol) for 2 h. Then the catalyst was regenerated by burning off the deposited coke under continuous flow of air at 823 K before the next test at 723 K and all other operating conditions are same.

Product analyses

Reaction products were analysed using Shimadzu 2014 Gas Chromatograph equipped with Flame Ionization Detector (FID) and a capillary column Stabilwax (60m-length, 0.32 mm ID, and 0.5 μm thickness of Polyethylene glycol stationary phase). The material balance based on carbon exceeded 95% and almost third of the catalytic runs were carried out two times to ensure reproducibility of the product compositions.

Results and Discussion

Diffusivity of xylene isomers viz a viz their distribution in product

Figure 1 shows the XRD patterns of parent and modified versions of zeolite Beta and confirms the integrity of the framework structure after desilication and subsequent silylation modifications.

Table 1 shows the values of surface- and bulk-Si/Al ratios determined by EDX and ICP-OES, respectively. Lower bulk Si/Al ratio for desilicated sample is in line with expectation. Lower surface Si/Al ratio for desilicated sample than that for the parent zeolite maybe because of Al enrichment of the surface after desilication¹¹. Lower value of surface Si/Al ratio for double silylated desilicated zeolite Beta sample (9.62) as compared to the parent sample (12.06) may be due to amorphous material deposition at the surface due to silylation¹² though bulk Si/Al did increase to 13.61.

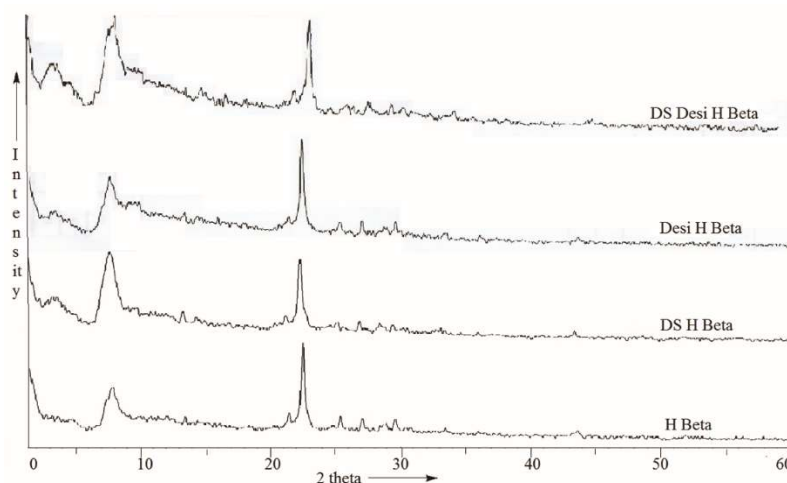


Fig. 1 — XRD patterns of various zeolite Beta samples

Table 1 — Si/Al Ratios of zeolite samples

Sample	EDX analyses	ICP-AES analyses
Parent	12.06	12.55
Desilicated	11.38	10.93
Double silylated desilicated	9.62	13.61

Hysteresis observed in nitrogen adsorption-desorption isotherms for parent zeolite Beta may be attributed to inter-crystalline voids. The width of hysteresis increases after desilication and decreases after silylation, both trends (viz a viz proportions of mesoporosity) agree with expectations. However, even after silylating desilicated zeolite Beta two times, it retained larger fraction of its mesoporosity. Table 2 shows the surface area and pore volume for different zeolite Beta samples. Desilication marginally increased area corresponding to mesopores. When parent zeolite Beta was silylated, area corresponding to micro- and meso-pores dropped (392 to 255 m²/g, and 118 to 67 m²/g, respectively). This observation indicates that the silylating agent employed in this work, TEOS, has entered the pores of zeolite Beta. The molecular size of TEOS is 10 Å¹³ whereas average pore size of zeolite samples is about 30 Å, Table 2. Similar trends were observed for desilicated zeolite Beta also (350 to 274 m²/g, and 120 to 75 m²/g). These trends are reflected in corresponding values for pore volume too. Further, BET micropore cross-section size did not vary much after two treatments. Thus, no pore narrowing effect could be realized by using TEOS as silylating agent. Figure 2 (A) depicts the CO₂ adsorption kinetics. Parent- and desilicated-zeolite Beta exhibited highest

uptake whereas for the silylated samples the CO₂ uptake was almost half of the former two cases. Now CO₂ being a small molecule, lower uptake for silylated zeolites suggests the reduction in micropore volumes. Thus the CO₂ adsorption uptake observations corroborate the conclusion drawn above with regard to TEOS entering pores of zeolite Beta unlike its preferential deposition on crystals' external surface as is the case with medium pore zeolite ZSM-5.

Figures 3(A) and 3(B) show toluene conversions at 673 K and 723 K, respectively. For all catalysts, conversions dropped with TOS, as also has been reported by Ahn *et al.*¹⁴ for zeolite Beta. Rates of deactivation of all catalyst samples were comparable at a given reaction temperature. Rates of deactivation at 723 K were lower than those at 673 K for corresponding catalysts. The deactivation can be attributed to coking arising from the oligomerization of olefins formed from methanol and multialkylated aromatic products, also. Thus, at higher temperature, more of methanol is consumed towards alkylation. Also, at higher temperature, toluene conversions were higher. However, xylene selectivity exhibited the reverse trend, Figs 3(C) and 3(D). Influence of the modifications of parent zeolite Beta is clearly discernible in Figs 3(A) and 3(B). Toluene conversion followed the trend, parent zeolite Beta < desilicated zeolite Beta ≈ single silylated desilicated zeolite Beta < double silylated desilicated zeolite Beta. This is in agreement with the expectation, because upon desilication relative proportion of Al per unit mass of zeolite increases leading to increased acidity (from 0.642 for parent zeolite Beta to 0.836 mmol NH₃/g for desilicated zeolite Beta)¹⁵. When desilicated zeolite

Table 2 — Textural properties of catalyst samples

	Parent H-Beta	Desilicated H-Beta	Double silylated H-Beta	Double silylated desilicated H-Beta
Surface area, m ² /g	510.9013	470.7157	322.9369	348.9883
BET Surface Area	392.3706	350.2392	255.6397	274.0638
t-Plot Micropore Area:	118.530	120.476	67.2972	74.9245
t-Plot External Surface Area:				
Pore volume, cm ³ /g	0.176136	0.155954	0.116021	0.122688
t-Plot micropore volume:	0.260953	0.245058	0.179697	0.166700
BJH Adsorption cumulative volume of pores between 17.000 Å and 3000.000 Å diameter:	0.258900	0.247249	0.178643	0.167082
BJH Desorption cumulative volume of pores between 17.000 Å and 3000.000 Å diameter:				
Pore size, Å	29.8834	30.0461	29.8399	27.9781
Adsorption average pore width (4V/A by BET)				
BJH Adsorption average pore diameter (4V/A)	93.039	86.592	113.059	94.530

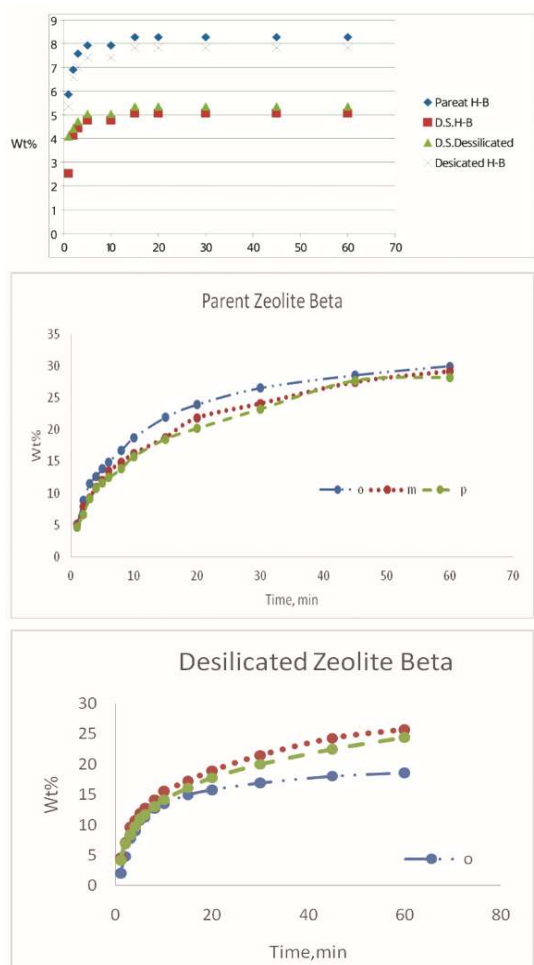


Fig. 2 — Adsorption kinetics (A) for CO₂ on various zeolite Beta samples; for xylene isomers on (B) parent and (C) desilicated Zeolite Beta. All at 298 K

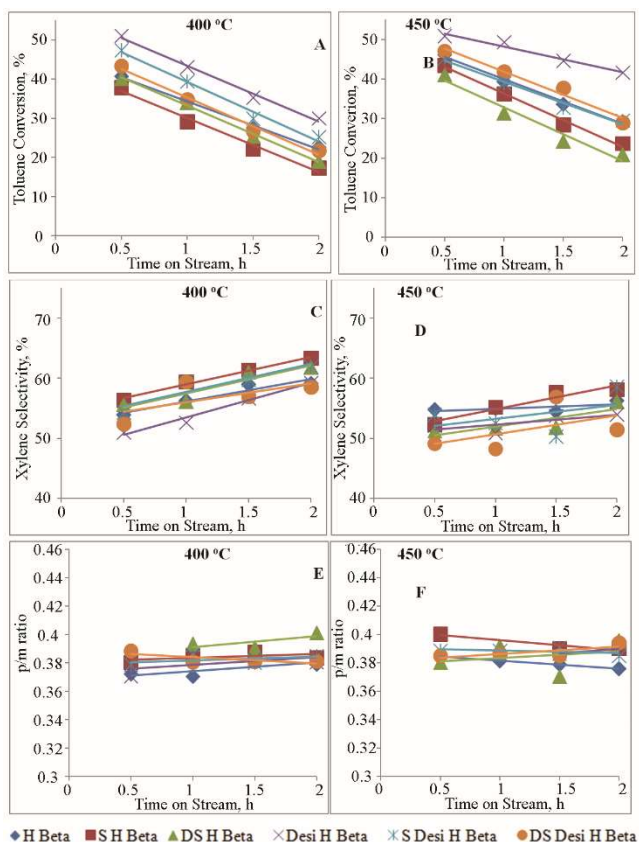


Fig. 3 — Performance parameters in toluene methylation, catalyst mass = 2 g, WHSV = 2.6 h⁻¹, Tol/MeOH = 6:1 mol/mol, H₂/HC = 2 mol/mol

Beta was silylated, toluene conversion dropped, though, still higher than that by parent zeolite. Only marginal reduction in toluene conversions after silylation of parent and desilicated zeolites imply that

very little pore narrowing could be realized. This is also reflected in hardly any increase in *para*-xylene selectivity. Variation in xylene formation with reaction temperature was mentioned above. At both temperatures, xylene selectivity, in general, increased with TOS. This increase is attributed to less toluene consuming side reactions, namely, toluene disproportionation and toluene dealkylation with TOS. Comparing trends seen in Figs 3(C) and 3(D), it is clear that rate of increase of xylene selectivity is lower at higher temperature, implying that toluene disproportionation and toluene dealkylation are suppressed at lower temperature. Figure 3 (C) gives information as to effects of change in zeolite's acidity caused by desilication and silylation on xylene selectivity. Taking parent zeolite as a base case, desilicated zeolite Beta gives minimum xylene selectivity, an attribute of increased acidity of the latter responsible for undesired toluene disproportionation and toluene dealkylation. Higher xylene selectivity with silylated parent zeolite can be attributed to blockage of some of the acid sites on the external surface where non-shape selective reactions, e.g., multialkylation can proceed. The same argument should hold good for the case of silylated desilicated zeolite beta samples which exhibit higher xylene selectivity than that by desilicated zeolite. Figures 3(E) and 3(F) show the values molar ratio of *para*- to *meta*-xylene in C₈ aromatics formed during the reaction. Thermodynamic distributions of xylene isomers at 700 K and 800 K indicate the values molar ratio of *para*- to *meta*-xylene to be 0.4526 and 0.4498, respectively¹⁶.

However, the observed values of this parameter hardly exceeded 0.4 on any of the catalysts studied. This means that more of *meta*-isomer formed than even thermodynamics dictate. In fact, value of this ratio as low as 0.08 for parent-, 0.45 for desilicated- and 0.52 for silylated desilicated-ZSM-5 can be calculated from the product distribution reported by Zhu *et al.*¹⁷ *Para*-selectivity afforded by zeolite ZSM-5 is chiefly explained based on higher diffusivity of the *para*-isomer against that of other two isomers by three order of magnitude. Now, observations of this work are rationalized based on xylene diffusivity values reported for various large pore materials. Masuda *et al.*¹⁸ had reported $D_{para-xylene} \approx D_{ortho-xylene}$ at 573 K on zeolite Y and Roque *et al.*¹⁹ had reported $D_{meta-xylene} = 1.44 D_{toluene} (\approx D_{para-xylene}) = 2.6 D_{ortho-xylene}$ at 450 K on zeolite Beta. As critical size size of *para*-xylene is equal to be that of toluene (Table 3) and hence their

diffusivity too²⁰, one expects that *meta*-xylene should have highest diffusivity among three isomers in large pore zeolites. Figures 2 (B and C) respectively show xylene adsorption kinetics over parent and desilicated zeolite Beta. Diffusivity values of xylene isomers determined (by PK and VLP appearing in Acknowledgement) at 298 K are summarized in Table 4. They clearly reveal that on parent zeolite Beta *para*-xylene diffusivity is only 1.34 times higher than that of *meta*-xylene whereas on mesoporous, desilicated zeolite Beta, this value is 1.33 !! Agreeing to the trend observed here, Ergun *et al.*²¹ also had reported comparable diffusivity of all three isomers of xylene in large pore material, MCM-41 and McQueen *et al.*²² in large pore (7.4 Å) steam- and then acid-treated zeolite mazzite possessing mesopores. Very recently Toda, *et al.*³⁰ have predicted the values of ratios of diffusivities of *para*- to *meta*-xylene and *para*-to *ortho*-xylene to be 0.45 to 2.55 and 1 to 3.8, respectively in 12-membered channels with dimensions of (4.4 to 7) × (6.8 to 9.7) of various siliceous zeolites. These values are close to those determined in this work. (Table 4). This is contradictory to the trend commonly reported^{1,23} for medium pore zeolite ZSM-5. Groen *et al.*²⁴ also observed an increase in diffusivity of neopentane by two orders of magnitude in mesoporous ZSM-5 against parent ZSM-5. Further, very recently Vattipalli *et al.*³¹ have shown that on hierarchical materials, the diffusion length greatly exceeds the crystal or particle size and

Table 3 — Xylene molecular size²³

Molecular size (nm)	Maximum	<i>para</i> -	<i>meta</i> -	<i>ortho</i> -	Toluene
		Xylene	Xylene	Xylene	e
		0.99	0.92	0.87	0.87
	Minimum (critical size)	0.67	0.74	0.73	0.67

Table 4 — Diffusivities of xylenes (d/r²), s⁻¹ x10⁵, d: diffusivity; r: equivalent radius of zeolite crystals

Zeolite	<i>para</i> - Xylene	<i>meta</i> - Xylene	<i>ortho</i> - Xylene	<i>para</i> -/ <i>meta</i> -	<i>para</i> -/ <i>ortho</i> -
Zeolite Beta	e	e	e	-	-
Parent	8.094	6.0454	7.8	1.34	1.03
Dealuminate	11.5	6.3845	7.3	1.80	1.59
d					
Desilicated	9.229	6.9396	9.9	1.33	0.93
Desilicated/ Parent	1.14	1.15	1.26	1.01	1.11

formed products diffusing out of micropores would diffuse through the mesopores and would re-enter the micropores once again. Thus, even if *para*-isomers might be initially forming, due to enhanced diffusion lengths within the crystals the xylene isomers would tend to attain the thermodynamic distribution. Forbye reported values of proton affinity of *meta*- and *para*-xylene are 195.9, and 192 kcal/mol³². They give an impression that the former would bind longer on zeolite acid sites and then converts to balance two isomers. However, this intuitive expectation would not be valid for weak bases, which xylene isomers *are*, in light of the observation by Patet *et al.*³³ "... the PA (proton affinity, added by the present author) of the adsorbate is not a reliable descriptor of the relative binding strength of molecules with weak basicity." Thus, important conclusions drawn from our catalytic- and adsorption kinetics- observations are (1) in large pore zeolites, difference in diffusivity values for large and small molecules is less than those in medium pore zeolites, and (2) in mesoporous materials, diffusivity of smaller molecule does not increase greatly to lead to enhanced *para*-selectivity. These disprove the claims of Yashima *et al.*⁴ of large pore zeolite affording *para*-selectivity, *para*-isomer being the primary product. Our results showed the molar ratio of *para*- to *ortho*-xylene in product to be about 0.89 to 0.98 for all the catalysts and at both reaction temperatures. This value varied from 0.61 on parent zeolite Beta²⁵ to 2.29 on zeolite HY⁴ i.e., high *para*-selectivity. Summarily, modifications attempted in the present work failed to afford *para*-selectivity, though desilication did enhance catalyst's activity.

Now, it is clear that toluene gets consumed by three parallel reactions: (i) toluene methylation to C₈ aromatics as products, (ii) toluene disproportionation to xylenes and benzene, and (iii) toluene dealkylation to benzene and methyl carbenium ions, the latter responsible for coke formation and hence catalyst deactivation. At high reaction temperatures employed in this work, 673 K and 723 K, utilization of large fraction of methanol is expected for alkylation reaction rather than olefin formation followed by their oligomerization and subsequent coke formation. As toluene to methanol molar ratio in feed was 6 and with the assumption that most of methanol is used for alkylation reaction, highest toluene consumed for single methylation is 16.6%. Extents of these reactions are determined as shown below.

Benzene: x

Toluene: y

C₈ aromatics: z

Toluene conversion = $100 - y$

Toluene conversion by alkylation = 16.6

Toluene conversion by disproportionation = $z - 16.6$

Toluene conversion by dealkylation = $x - (z - 16.6)$

Analysis of catalytic performance

Figures 4 and 5, respectively depict the extents of different reactions calculated from product distribution for silylated parent- and silylated desilicated- zeolite Beta samples. It is to be noted that toluene conversion by methylation is constant for all the cases at 16.6% and in this context, TOTAL toluene conversion is shown in Fig 4 and 5. In these figures, advantages of desilication in terms of increased toluene conversion and decreased deactivation rates are clearly visible. With desilication, number of acid sites per unit mass of zeolite increases and it takes relatively longer to occupy them by coke precursors as compared to parent zeolite Beta. It is pertinent to note that toluene

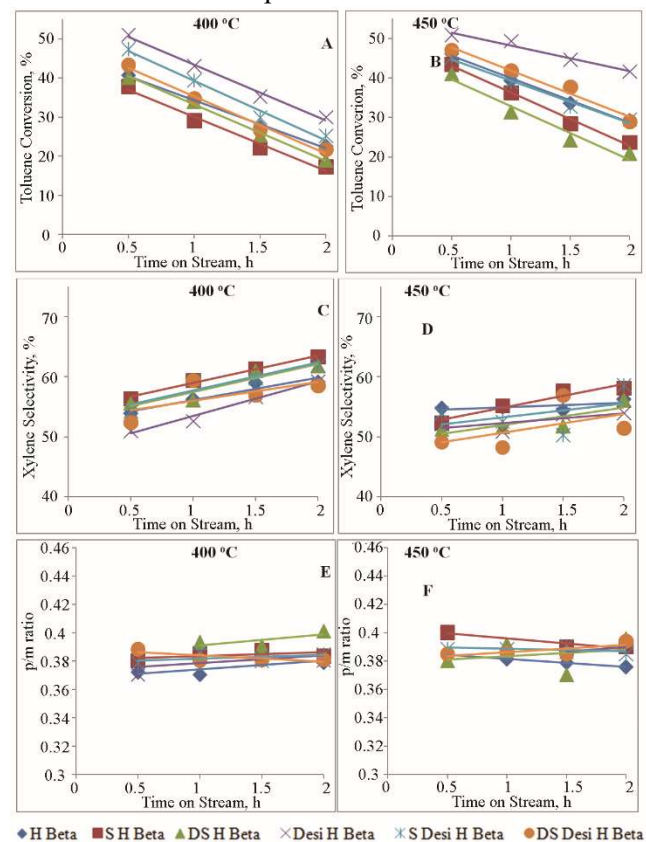


Fig. 4 — Extents of different reactions on silylated zeolite eta samples. Catalyst mass = 2 g, WHSV = 2.6 h⁻¹, Tol/MeOH = 6:1 mol/mol, H₂/HC = 2 mol/mol

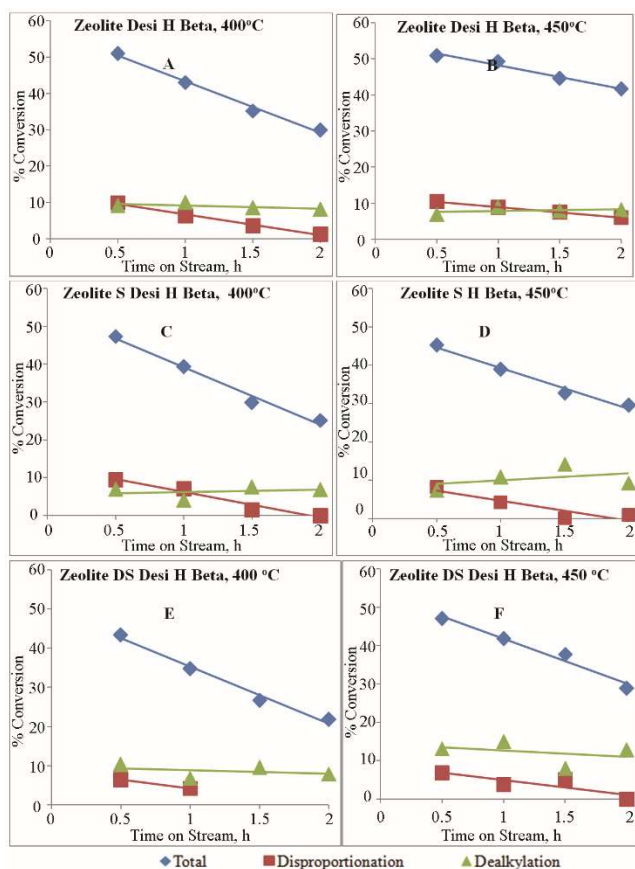


Fig. 5 — Extents of different reactions on silylated desilicated zeolite Beta samples. Catalyst mass = 2 g, WHSV = 2.6 h⁻¹, Tol/MeOH = 6:1 mol/mol, H₂/HC = 2 mol/mol

conversion by dealkylation remained almost constant with TOS and varied in a narrow range of $\pm 2\%$ of average value of 10% across all the catalysts. This conversion slightly increased with temperature as can be expected. Constancy of toluene conversion by dealkylation indicates that this reaction does not take place on strong acid sites that are the preferred location of coke formation. Extent of toluene disproportionation was least among all the reactions and it diminished to zero conversion by 1 h of TOS on silylated parent and desilicated zeolite Beta samples. This value for desilicated versions was 2 h, which again can be rationalized based on increased number of acid sites upon desilication.

Conclusion

Large pore zeolite Beta holds a promise as an efficient catalyst for toluene methylation reaction with increased rate of overall alkylation reaction, particularly when mesoporosity has been generated in it. Zeolite sample with mesopores afforded higher toluene conversion and exhibited lower rate of

deactivation. However, to impart *para*-selectivity narrowing down the pore openings is called for. Nonetheless, for this purpose, tetraethyl ortho-silicate would not serve the purpose. In the present work, proportion of *meta*-xylene was higher than that dictated by thermodynamics at reaction temperature. This could be explained on the basis of xylene isomer diffusivity in large pore zeolites of which trend is contrary to that in medium pore zeolite ZSM-5. Diffusivity of larger *meta*-xylene molecule seems to be higher than that of smaller *para*-xylene molecule in mesoporous zeolite Beta. Indeed, due to higher extent of toluene methylation reaction as compared to other toluene-consuming reactions, catalysts in the present study do meet one of the approaches acceptable to the industry: “The materials are first converted into mixtures of xylenes by an aromatic interconversion process, and then *para*-xylene is extracted”²⁶. This becomes more pertinent in light of the facts that catalyst deactivation is a major issue to be addressed in toluene methylation²⁷ as also was seen in the present study. One of the measures that has been resorted to is carrying out this reaction in fluidized bed²⁸ or moving bed reactor²⁹. In this context, it is not incorrect to envisage that zeolite Beta (particularly with its narrowed pore openings on crystal surface) may outperform in fixed bed mode which is easier to operate at the commercial scale.

Acknowledgement

Author thanks Mr. Rohit Kudtarkar for carrying out experiments and preparing Figures. Thanks are due to Dr. HC Bajaj of Central Salt and Marine Chemicals Research Institute, Bhavnagar, India for EDX and ICP-AES analyses. Thanks are also due to Prof. KK Pant of IIT Delhi, Delhi for kindly getting analyses done for pore size, surface area and pore volume of modified zeolite samples. Thanks are also due to Dr. Prakash Kumar and Dr. Vijaya Laxmi Puranik of RIL, Baroda for xylene adsorption kinetics study including diffusivity determination and many helpful discussions.

Nomenclature

H Beta: Parent Zeolite Beta

SH Beta: Silylated Zeolite Beta

DSH Beta: Double Silylated Zeolite Beta

Desi H Beta: Desilicated Zeolite Beta

S Desi HBeta: Silylated Desilicated Zeolite Beta

DS Desi HBeta: Double Silylated Desilicated Zeolite Beta

$D_{meta-xylene}$ = Diffusivity of *meta*-xylene

References

- 1 Ahn J H, Kolvenbach R, Al-Khattaf S S, Jentys A & Lercher J A, *Chem Comm*, 49 (2013a) 10584.
- 2 Al-Khattaf S S, Ali S A, Osman M S & Aitani A M, *J Ind Eng Chem*, 21 (2015) 1077.
- 3 Bhat Y S, Das J, Rao K V & Halgeri A B, *J Catal*, 159 (1996) 368.
- 4 Yashima T, Ahmad H, Yamazaki K, Katsuta M & Hara N, *J Catal*, 16 (1970) 273.
- 5 Al-Khattaf S, Rabiou S, Tukur N & Alnaizy R, *Chem Eng J*, 139 (2008) 622.
- 6 Chun Y, Chen X, Yan A & Xu Q, *Stud Surf Sci Catal*, 84(1994) 1035.
- 7 Chu S & Chen Y, *Ind Eng Chem Res*, 33 (1994) 3112.
- 8 Kunkeler P J, Moeskops D & Van Bekkum H, *Microporous Mater*, 11 (1997) 313.
- 9 Halgeri A B & Das J, *J Appl Catal A: Gen*, 181 (1999) 347.
- 10 Das J, Bhat Y S & Halgeri A B, *Ind Eng Chem Res*, 33 (1994) 246.
- 11 Fernandez C, Stan I, Gilson J, Thomas K, Vicente A, Bonilla A & Perez-Ramirez J, *Chem: Eur J*, 16 (2010) 6224.
- 12 Gil B, Mokrzycki L, Sulikowski B, Olejniczak Z & Walas S, *Catal Today*, 152 (2010) 24.
- 13 Niwano M, Simons J K, Frigo S P & Rosenberg R A, *J Appl Phys*, 75 (1994) 7304.
- 14 Ahn J H, Kolvenbach R, Al-Khattaf S S, Jentys A & Lercher J A, *ACS Catal*, 3 (2013b) 817.
- 15 Modhera B K, Chakraborty M, Bajaj H C & Parikh P A, *Catal Lett*, 141 (2011) 1182.
- 16 Albery R A, *J Phys Chem Ref Data*, (1985) 177.
- 17 Zhu X, Lobban L L, Mallinson R G & Resasco D E, *J Catal*, 271 (2010) 88.
- 18 Masuda T, Fukada K, Fujikata Y, Ikeda H & Hashimoto K, *Chem Eng Sci*, 51 (1996) 1879.
- 19 Roque R M, Wendelbo R, Mifsud & Corma A, *J Phys Chem*, 99 (1995) 14064.
- 20 Reitmeier S J, Gobin O C, Jentys A & Lercher J A, *J Phys Chem C*, 113 (2009) 15355.
- 21 Ergün A N, Kocabaş Z O, Yürüm A & Yürüm, Y, *Fluid Phase Equilibria*, 382 (2014) 169.
- 22 McQueen D, Fajula F, Dutartre R, Rees L V C & Schulz P, *Stud Surf Sci Catal*, 84 (1994) 1339.
- 23 Choudhary V R, Nayak V S & Choudhary T V, *Ind Eng Chem Res*, 36 (1997) 1812.
- 24 Groen J C, Zhu W, Brouwer S, Huynink S J, Kapteijn F, Moulijn J A & Pe' rez-Ram' rez J, *J Am Chem Soc*, 129 (2007) 355.
- 25 Llopis F J, Sastre G & Corma A, *J Catal*, 227 (2004) 227.
- 26 Gentry J C, www.digitalrefining.com/article/1001045, January 2015, 1.
- 27 Ghosh A K, Juttu G & Harvey P, US Patent 7060644, 2006.
- 28 Johnson D L, Tinger R G, Ware R A & Yurchak S, US Patent 6642426, 2003.
- 29 Gonçalves J C & Rodrigues A E, *Chem Eng Technol*, 39(2) (2016) 225.
- 30 Toda J, Corma A & Sastre G, *J Phys Chem C*, 2016.
- 31 Vattipalli V, Qi X, Dauenhauer P J & Fan W, *Chem Mater*, 28 (2016) 7852.
- 32 Lias S G, Liebman J F & Levin R D, *J Phys Chem Ref Data*, 13 (3) (1984) 695.
- 33 Patet R E, Caratzoulas S & Vlachos D G, *Phys Chem Chem Phys*, 18 (2016) 26094.